

Precipitation fields over the Baltic Sea derived from ship rain gauge measurements on merchant ships

Marco Clemens and Karl Bumke

Institut für Meereskunde Kiel, Düsternbrooker Weg 20, D-24115 Kiel, Germany

Clemens, M. & Bumke, K. 2002: Precipitation fields over the Baltic Sea derived from ship rain gauge measurements on merchant ships. — *Boreal Env. Res.* 7: 425–436. ISSN 1239-6095

Precipitation over the Baltic Sea has been estimated from satellite measurements, ground-based weather radars and synoptic observations made at coastal and island stations. The obtained estimates do not use any *in situ* measurements over the Baltic Sea. Thus, a validation of the estimates over the sea proper is required. Here we present a method to analyse precipitation measurements over the Baltic Sea from the ship observations for the period 1996–2000. In order to measure precipitation over the Baltic Sea, several merchant ships have been equipped with specially designed ship rain gauges. The measurements are stored at 8-minute intervals. More than 20 000 instrumental measurements were collected during several months. An interpolation scheme based on the kriging method has been used to estimate spatial precipitation distributions on a $1^\circ \times 1^\circ$ grid. This method is particularly used to minimise sampling errors due to the low data density. All estimations are presented on a seasonal time resolution. The estimated spatial rain fields give reasonable results, especially in areas along the main shipping routes characterised by a high data density.

Introduction

The oceans comprise more than 70% of the surface of the Earth. The precipitation over the oceans is crucially important for the estimation of its fresh water balance. During the recent years many efforts have been undertaken to investigate the spatial and temporal distribution of the precipitation over the sea. Since only a small number of *in situ* precipitation measurements are available over the sea, Tucker (1961) has introduced a method to derive precipitation rates from the present weather code massively

available in VOS (Voluntary Observing Ship) data. However, the Tucker's method, derived from land-born observations, results in large uncertainties and has been insufficiently validated so far. Although this method has frequently been used in the past to estimate the precipitation over the sea (e.g. Reed and Elliot 1973, 1977), it is unclear whether it can be applied on a global scale. Reed and Elliot (1973, 1977) showed that the Tucker's method gives reasonable results in extra-tropical regions, but fails in the tropics where further evaluation has been found to be necessary. Dorman and Bourke (1978) selected

28 coastal stations located along the coasts of the North Atlantic and Pacific Ocean, as well as several island stations. They found significant biases highly correlated with the air temperature in the Tucker's method. Finally, they developed a correction procedure to minimise these biases. Vermehren (1995) made another parameterisation for the precipitation rates for different present weather codes. Her relationships were based on the observations of the present weather and precipitation data onboard the German light vessels.

Further analyses of the spatial rainfall distributions over the sea have been derived from satellite and land-borne radar measurements and numerical weather prediction models. However, Simmer (1996) pointed out that the estimation of precipitation by remote sensing methods is still under development and needs further improvements. Present satellite retrieval algorithms perform better in locating precipitating clouds, whereas the estimation of precipitation amounts remains rather inaccurate. Large-scale numerical models generally overestimate the precipitation over the Baltic Sea (Omstedt *et al.* 2000). Regional models with a higher spatial resolution (e.g. REMO) demonstrate, similar to observations, spatial patterns of precipitation but give quantitative biases in the precipitation amounts (Rubel 1998). Radar measurements (e.g. those of the Swedish Weather Service (SMHI)) represent another useful source of precipitation data with high spatial and temporal resolution (Michelson *et al.* 2000a). However, land-based radar give sometimes unusually high rainfall amounts in the Baltic Sea proper due to the appearance of ground clutters, especially under a stable atmospheric stratification.

Despite the high resolution in space and time, all data sources described above suffer from the lack of verification of the precipitation estimates against *in situ* measurements. In contrast to these data, instrumental measurements are considered to be superior with respect to the observational error. Nevertheless, the conventional gauge precipitation measurements from the moving platforms (ships) are influenced by the impact of the ship's superstructure on the atmospheric flow, which induces spurious vertical velocities and enhances or reduces wind speeds at the location of the gauges, resulting in either an

undercatch or overcatch of the measured precipitation. The largest biases are associated with the wind-dependent undercatch due to the flow around the rain gauge under high wind speeds. It is important that wind-induced errors have a tendency to increase with increasing rain gauge sizes and strongly depend on the exposure of instruments (WMO in Reed and Elliot 1977). To address these problems, a new ship rain gauge (Hasse *et al.* 1998) and a new optical disdrometer (Großklaus *et al.* 1998) have been developed at the Institute for Marine Research at the University of Kiel.

The ship rain gauge

The ship rain gauge is designed to measure rain under high wind speeds as they occur on moving ships. An outstanding feature of the ship rain gauge used is an additional lateral collector (Fig. 1) which is effective especially under high wind speed conditions (Hasse *et al.* 1998). Conventional cylindrical gauges tend to shift the rain above the orifice of the gauge under high wind speeds, resulting in a massive underestimation of present rainfall. The ship rain gauge catches additionally the water that has been transported from the lateral environment. Being based on the water amounts collected from the top and lateral, and considering the wind speed relative to the instrument, it is possible to derive the true rainfall. For this purpose, in the Hasse *et al.* (1998) rain gauge the amount of rain is estimated for each collector separately. For low wind speeds the catchment of the precipitation at the top of the instrument is quite accurate and only a small correction is required. At high wind speeds when the impulse of rain drops is nearly horizontal, the measurements at the lateral collector lead to the least biased estimate of the rainfall, while the measurements at the upper collector require an extensive correction due to the undercatch (Hasse *et al.* 1998). Finally, a wind-speed-dependent algorithm is used to estimate the true rainfall from both the upper and lateral collector. In this algorithm a linear transformation is used to weight the estimated rainfall rates at the top and lateral collector for the wind speed range 9–11 m s⁻¹.

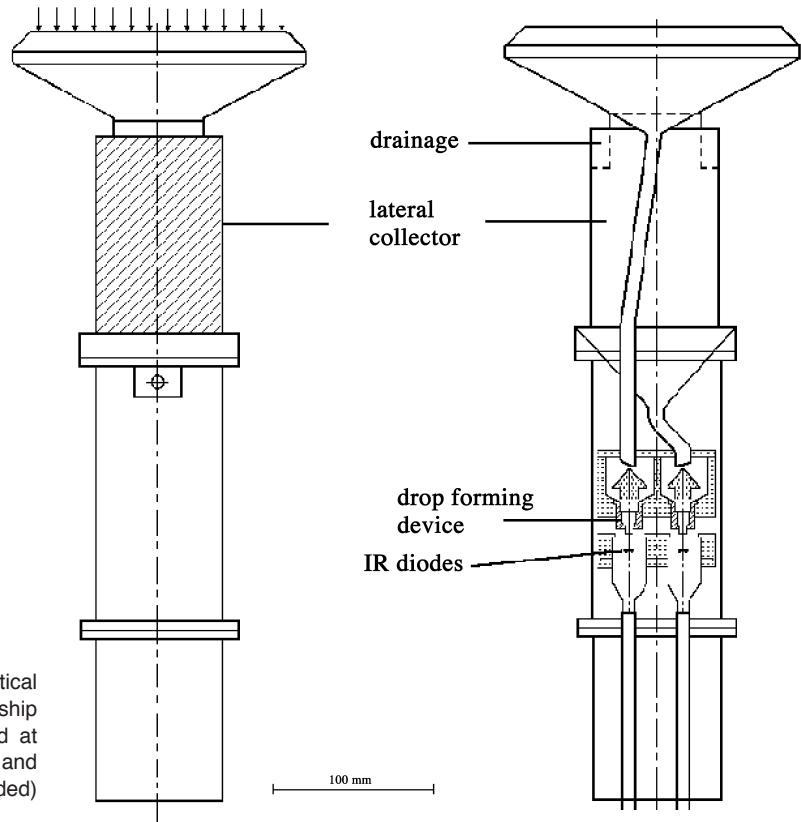


Fig. 1. Side view (left) and vertical cross section (right) of the ship rain gauge. Rain is collected at the horizontal orifice (arrows) and at the lateral collector (shaded) (Hasse 1998).

Calibration and verification

We performed a new calibration of the ship rain gauge during simultaneous measurements with an optical disdrometer onboard *r/v Alkor* between 1999 and 2001. The uncertainties associated with wetting and evaporation were taken into account during the calibration. The correlation between the two data sets was very high with a coefficient equal to 0.96. Hasse *et al.* (1998) gave an estimate of the relative standard error of the ship rain gauge of 2.4% for the hourly means. They also noticed that 6-hour or daily totals are even more stable. We can mention in this context the estimates of Skomorowski *et al.* (2001), who gave error estimates in the range of 20% for satellite measurements (GPCP-1DD) made in the area of the alpine alps. Calibrations of the GPCP-1DD data against measurements from a very dense gauge network (Frei and Schär 1998) showed that the accuracy of the GPCP-1DD precipitation is comparable to other satellite estimates. We verified the precipitation

measurements from the ship rain gauge against several conventional gauges.

A comparison of the daily precipitation amounts measured by the ship rain gauge and a Hellmann rain gauge on the top of the roof of the Institute for Marine Sciences (University Kiel) was done for the period 1996–2001 (Fig. 2). To exclude the days with solid precipitation, we used only data from the days with air temperatures above 4 °C. In the comparison we used exclusively the precipitation data from the dates for which records from both the instruments were complete. Measurements of the Hellmann gauge were corrected to account for the wind speed, wetting loss, and evaporation according to Rubel and Hantel (1999). The correlation coefficient between the daily amounts derived was equal to 0.97. The total sum of precipitation measured by the ship rain gauge was 1184 mm, while the Hellmann gauge gave 1120 mm. The standard deviation of the measurements made by the ship rain gauge (2.18 mm day⁻¹) was somewhat higher than that measured by the Hellmann rain gauge

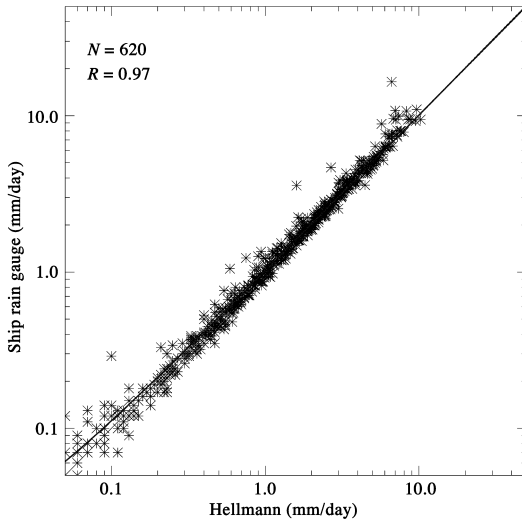


Fig. 2. Comparison of daily precipitation amounts measured by the ship rain gauge and the Hellmann on the roof of the Institute for Marine Science during the Period 1996 till 2001.

(1.81 mm day^{-1}). In order to estimate the spatial distribution of precipitation over the Baltic Sea, several observing ships have been equipped with ship rain gauges. This activity was launched in 1994 at ships travelling between Lübeck (Germany) and Helsinki (Finland) through the southern and central Baltic Sea (Fig. 3). The instruments were properly installed onboard at sites in which the flow is nearly horizontal. The relative wind speed measurements were taken from the same positions in order to correct the rain gauge measurements.

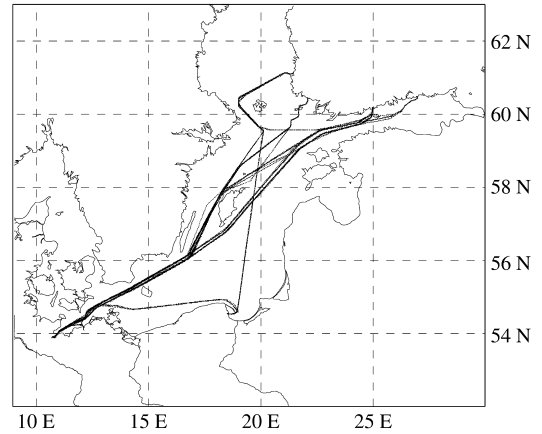


Fig. 3. Cruises of the voluntary observing ships equipped with ship rain gauges during autumn 1998.

The rain measurements were typically stored at 8-minute intervals, which allows minimising the influences of fast-travelling ships on the measurements and makes it possible to consider samples as point measurements. The measurements were randomly distributed in time and space along the shipping routes (Fig. 3). The total number of the collected measurements exceeded 20 000 during several months (Fig. 4). For the further analyses, the winter seasons were excluded to avoid the treatment of snow, which is not effectively measured by the instrument. Rutgarsson *et al.* (2001) estimated the accumulated precipitation over the Baltic Sea Proper during a part of the PIDCAP period (Isemer 1996) using five different data sources.

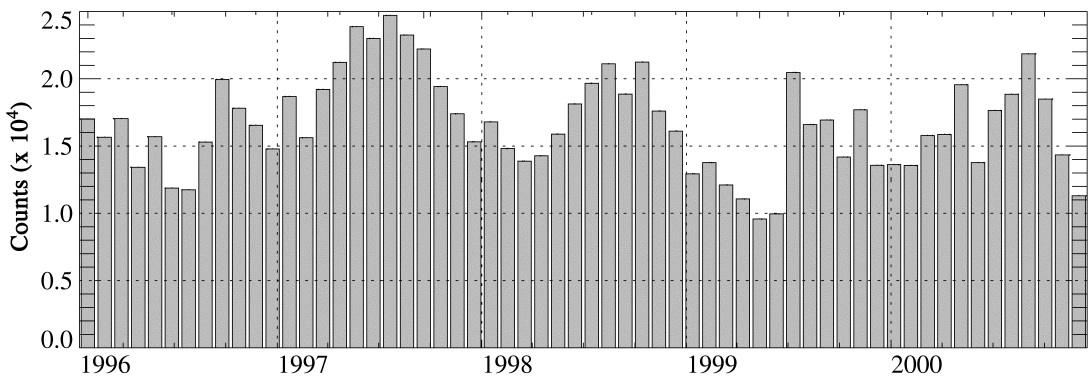


Fig. 4. Number of monthly available ship rain gauge measurements from voluntary observing ships during the period 1996 till 2000.

These were the analyses of the Swedish Mesoscale Analysis System MESAN (Michelson *et al.* 2000b) that is based on synoptic observations and the Baltic radar data, the SMHI(1×1)° data base that have been gridded by using an optimal interpolation of precipitation measurements, precipitation estimates based on the COADS data (Ismer and Lindau 1998), and SSM/I (Special Sensor Microwave/Imager) precipitation data. In comparison to the ship rain gauge measurements (128 mm), the analyses of MESAN and SMHI(1×1)° reported an overestimation of about 9% in the accumulated precipitation, while COADS and SSM/I data tended to underestimate the total amount of precipitation by 22% during this period.

Method of the spatial analysis of precipitation measurements

During the recent years, several different methods have been used to analyse the spatial and temporal variability of precipitation. A short description of some of these techniques has been given in Hall and Barclay (1975). Creutin and Obled (1982) made an objective comparison of six different methods. They separated six analysis procedures into two classes, one of which was based on a relatively simple statistics. The other class of procedures used more advanced statistical methods such as the optimal interpolation (Gandin 1965), kriging (Matheron *et al.* 1963), or the reconstruction of empirical orthogonal functions (EOF) (Obled and Creutin 1986). To analyse the precipitation measured by the ship rain gauges over the Baltic Sea, we derived a procedure based on the kriging method as described by Bacchi and Kottogoda (1995) and Rubel (1996). We modified the original method by performing a Monte Carlo generation of the sampling error. The procedure starts with the analysis of all *in situ* precipitation measurements (Fig. 5), which serve as input for estimating the sampling errors, mean fields and spatial correlation functions on a 8-minute timescale. The next step is to obtain first-guess precipitation fields from the analysed data, and to derive spatial correlation functions on a seasonal timescale. The averaged fields based on the raw measure-

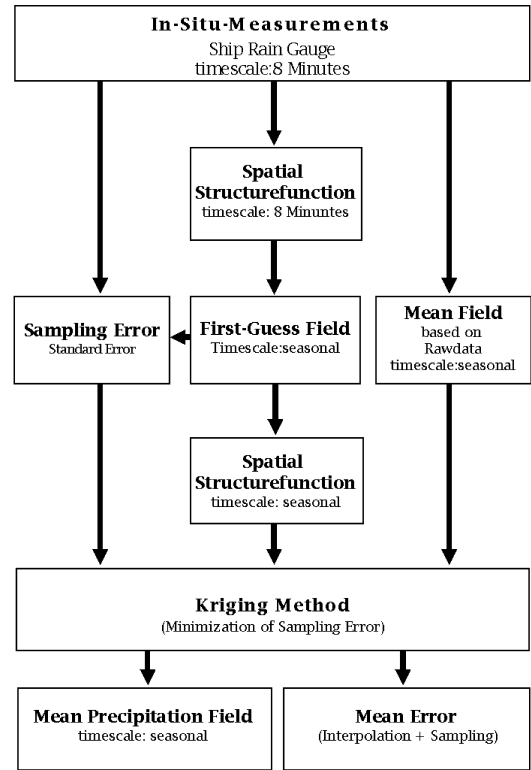


Fig. 5. Overview of the procedure of the precipitation analyses based on the ship rain gauge measurements.

ments, sampling variance estimates and spatial structural functions constitute the input for a main analysis procedure. The outcome of the technique consists of gridded fields produced by kriging, which is tuned to the estimated sampling variances and characterised by the interpolation error quantified by a so-called kriging variance. A more detailed description of the analyses will be given in the following sections.

Averaged fields of the raw data

To obtain an initial estimate for the spatial fields of precipitation from the measured rain rates (rr), the gridded values were derived on a $1^\circ \times 1^\circ$ grid on a seasonal timescale. For this purpose, all 8-minute measurements rr 's within a grid box were averaged implementing for the mixed lognormal distribution of the data analysed its continuous part at $rr = 0.0 \text{ mm h}^{-1}$ and the discrete lognormal part for $rr > 0.0 \text{ mm h}^{-1}$ (Kedem *et al.* 1990). The

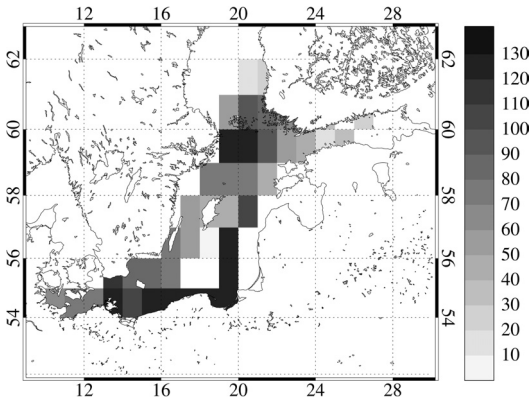


Fig. 6. Arithmetic averaged precipitation for autumn (September–November) 1998 derived from 8 minutes measurements of the ship rain gauges. Units are mm month^{-1} .

means $E(rr)$ and the variances $\text{Var}(rr)$ were calculated from the distribution of the data according to Aitchison and Brown (1963):

$$E(rr) = p \exp\left(\mu + \frac{\sigma^2}{2}\right), \quad (1)$$

$$\text{Var}(rr) = p \exp(2\mu + \sigma^2)(\exp\sigma^2 - p), \quad (2)$$

where μ denotes the mean of the transformed data, σ stands for the corresponding standard deviation for all measurements with $rr > 0.0 \text{ mm h}^{-1}$, and p is the estimated rainfall probability. An example of the averaged rain field for the period September–November 1998 gave an averaged rain rate that ranged from 30 mm month^{-1} near Finland to $110 \text{ mm month}^{-1}$ in the south-east part of the Baltic Sea (Fig. 6). A common feature for the derived seasonal fields was a high level of spatial variance. These variances can partly be explained by a low number of samples of measured precipitation in individual grid boxes. This effect results in a so-called sampling error and has to be considered separately. The data density for each grid box varied from 20 measurements per grid box in poorly sampled areas to more than 8000 measurements per grid box near the coasts of Germany and Finland. A typical frequency of precipitation was between 5% and 14% (Fig. 7). Considering the maximum rainfall in the south-eastern part of the Baltic Sea, this estimate agrees with a minimum sample size in the corresponding grid boxes of the field of observational

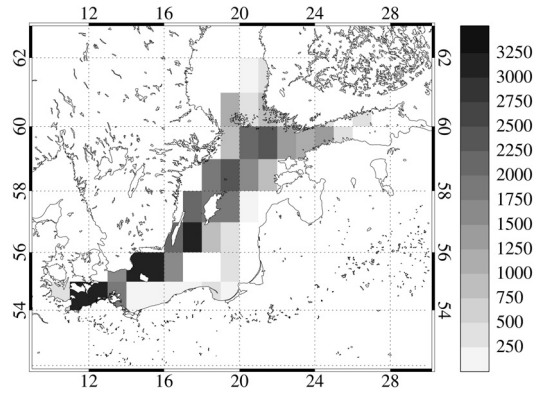


Fig. 7. Number of ship rain gauge measurements per grid box for autumn 1998.

density (Fig. 7). Therefore, the seasonal means in these areas were influenced strongly by the small number of measurements and, consequently, they were not statistically significant.

First-guess fields

The estimation of means (as given in the previous section) is based exclusively on information from a given grid box. More reliable results can be obtained if additional information about environmental effects is used. In this case, the amount of used information used increases and therefore the estimated means become more stable. The impact of this supplementary information has been quantified using the spatial statistics of precipitation processes. Thus, the first-guess fields were estimated by the use of weighted averages. The weights were chosen as functions of the distance between every individual measurement and the centre of the analysed grid box. Then the spatial structure functions for the precipitation measurements at different points were calculated using the standardised correlation coefficients. To identify an appropriate model for the autocorrelation function, simultaneous measurements were grouped into classes of pairs separated by a prescribed distance. The correlation coefficients derived for each distance class allow for the computation of empirical autocorrelation functions. These functions were based on 8-minute measurements made during each season and account for the nonlinearity associated with a

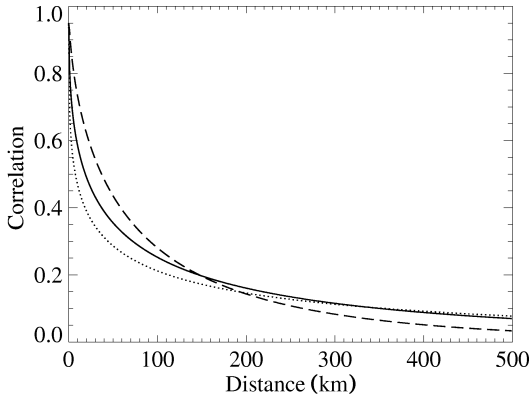


Fig. 8. Climatological spatial correlation functions for the seasons spring (March–May, solid line), summer (June–August, dashed line) and autumn (September–November, dotted line). The functions are based on the 8 minutes measurements of the ship rain gauges from 1996 to 2000.

seasonal variability in the rain. This analysis implies the assumption that the correlation function is constant for each season. Thus, the method actually deals with a mixture of different processes, represented for instance by the frontal and convective rainfall. To achieve the stability of spatial statistics, the structure functions were estimated for the climatological seasons. This procedure allows us to minimise the impact of mixed lognormal distributions and the limited number of measurements.

The averaged autocorrelation functions for spring, summer and autumn were derived from the measurements during 1996–2000 (Fig. 8). As a measure of the effectiveness of autocorrelation functions, a decorrelation length has been estimated. It has been defined as the distance at which the correlation decreases to the value of $1/e$. The functions adapted from measurements made during the spring and summer gave the largest decorrelation lengths of 46 and 68 km, respectively. This indicates a predominant stratiform or frontal precipitation, whereas a shorter decorrelation length in the autumn (~ 25 km) is an indicator of a convective rain.

In order to interpolate the ship rain gauge data, every single measurement was weighted with the value of the autocorrelation function, referring to its distance from the centre of every grid box. According to the distribution charac-

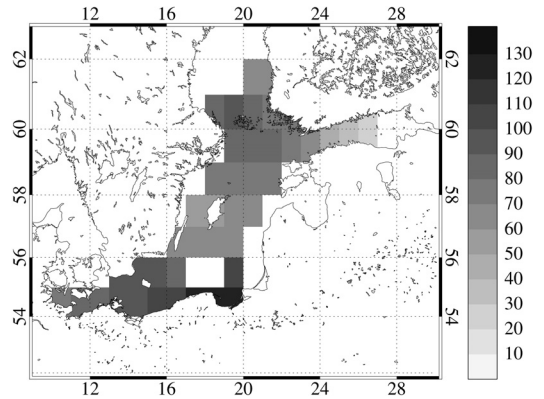


Fig. 9. First guess field of precipitation for autumn 1998 based on ship rain gauge measurements according to Eq. 3. Units are mm month^{-1} .

teristics of ship rain gauge measurements, the transformed means μ and variances σ^2 were calculated as

$$\mu = \frac{\sum_{i=1}^{n_{rr}} [\lambda_{rr,i} \ln(rr_i)]}{\sum_{i=1}^{n_{rr}} \lambda_{rr,i}}, \quad (3)$$

$$\sigma^2 = \frac{n_{rr} \sum_{i=1}^{n_{rr}} \left\{ \lambda_{rr,i} [\ln(\lambda_{rr,i}) - \mu]^2 \right\}}{(n_{rr} - 1) \sum_{i=1}^{n_{rr}} \lambda_{rr,i}}, \quad (4)$$

$$p = \frac{\sum_{i=1}^{n_{rr}} \lambda_{rr,i}}{\sum_{i=1}^{n_{rr}} \lambda_{rr,i} + \sum_{j=1}^{n_0} \lambda_{0,j}}, \quad (5)$$

where n_{rr} is the number of measurements rr_i with $rr > 0.0 \text{ mm h}^{-1}$, n_0 is the number of measurements with $rr = 0.0 \text{ mm h}^{-1}$, and λ_i are the corresponding weights. The resulting estimates for the means $E(rr)$ and the variances $\text{Var}(rr)$ were calculated according to Eqs. 1 and 2.

In comparison to purely arithmetically averaged fields, the first-guess fields are more smoothed in space and displayed a completely different behaviour in some areas (Fig. 9). The local extreme values are sometimes less pronounced and often widely stretched in their spatial extent. That is the case in the vicinity of the Ålands. On the other hand the area with highest precipitation rates in the south-eastern Baltic

shrinks. The differences in the behaviour of the local extremes can be described by large differences in a local data density. Therefore, a qualitative description of the weighted fields in terms of sampling error estimates could not be performed. But we can argue that the error magnitude has been significantly minimised after the implementation of the supplementary information.

Minimisation of the sampling error by kriging

In order to get reliable estimates of seasonal precipitation fields, we used kriging which accounts for a sampling error statistics. In principle the kriging method allows for a determination of the production of regular spatial fields from randomly distributed measurements. With the assumption that the precipitation field is homogeneous and isotropic, the true value of precipitation can be estimated by taking the integral of all precipitation processes $Z(\mathbf{u})$ located in the surrounding area A at $\mathbf{u} \equiv (x,y)$:

$$Z(\mathbf{u}_a) = \frac{1}{A} \int_A Z(\mathbf{u}) dx dy. \tag{6}$$

If the spatial structure function (in our case the autocovariance or the correlation function) is known, the unknown true precipitation value \hat{Z} at a point \mathbf{u}_a can be derived from a linear combination of the weights λ_i and the random values of the considered process $Z(\bullet)$.

$$\hat{Z}(\mathbf{u}_a) = \sum_{i=1}^n \lambda_i [Z(\mathbf{u}_i) + \delta(\mathbf{u}_i)]. \tag{7}$$

The error $\delta(\mathbf{u}_i)$ in the Eq. 7 can be described as a “white-noise” random process, which is determined mainly by a sampling error associated with the data density. If the estimates are assumed to be unbiased, the mathematical expectations of the estimate and true precipitation value should be equal to each other:

$$E[\hat{Z}(\mathbf{u}_a)] = E[Z(\mathbf{u}_a)]. \tag{8}$$

In addition, the condition of a minimum variance should be satisfied (i.e. the variance of the estimates from all realisations should be a minimum with respect to their weights):

$$\text{Var}[\hat{Z}(\mathbf{u}_a)] = E[Z(\mathbf{u}_a) - \hat{Z}(\mathbf{u}_a)]^2 = \sigma_E^2(\mathbf{u}_a), \tag{9}$$

$$\sigma_E^2(\mathbf{u}_a) = \min. \tag{10}$$

The minimised expression then gives an estimate for the variance, quantifying the mean square interpolation error of the estimated value:

$$\begin{aligned} \sigma_E^2(\mathbf{u}_a) = & \rho(\mathbf{u}_a) - 2 \sum_{i=1}^n \lambda_i \rho(\mathbf{u}_a, \mathbf{u}_i) \\ & + \sum_{i=1}^n \sum_{j=1}^n \lambda_i \lambda_j \rho(\mathbf{u}_i, \mathbf{u}_j) \\ & + \sum_{i=1}^n \lambda_i \delta(\mathbf{u}_i)^2. \end{aligned} \tag{11}$$

The first term in Eq. 11, the so-called kriging variance, denotes the variance at point \mathbf{u}_a . The second term comprises the covariances between the point for which the prediction is derived and the surrounding points. It accounts for information about the data point and allows for the reduction of the error. The third term describes the redundancy between the data points in the surroundings. The influence of the sampling error is given by the last term. To calculate seasonal precipitation fields from the ship data, a parameterisation for the sampling error $\delta(\mathbf{u}_i)$ and a spatial structure function on a seasonal timescale are required.

Sampling error statistics

The treatment of precipitation processes on the basis of measurements requires the consideration of the different errors that influence the analysis technique. Typical error sources inherent into the analysis are the following:

- random observational measurement error,
- random sampling error,
- non-random sampling fair weather bias,
- interpolation error present in the unsampled locations.

The random sampling error explains the major part of the cumulative error source. Thus, the estimation of the sampling error due to undersampling is mostly important to a realistic determination of the spatial precipitation distri-

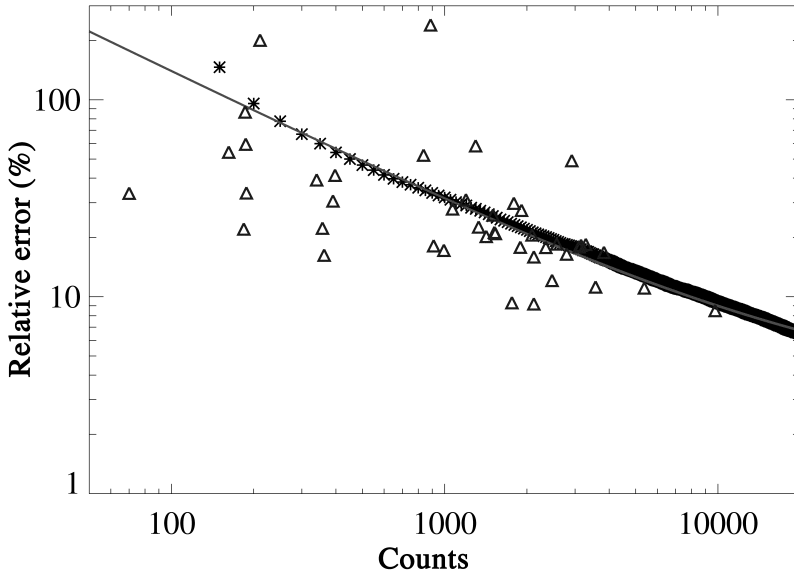


Fig. 10. Averaged relative error (%) as a function of the number of measurements for autumn 1998. Crosses denote the results of the Monte Carlo simulations while the line is a estimated empirical function. Triangles are the corresponding errors estimated by Monte Carlo simulations based on means and variances according to the corresponding first guess field for the same period.

bution. Thereby, the sampling error depends on the characteristics of the statistical distribution of measurements. Since the parameters of a mixed lognormal distribution are not known for every single grid point, the estimated values of the first-guess fields were taken as a starting point. These parameters describe the shape of the probability distribution and have to be estimated for each grid point separately due to the impact of the spatial variability of the mean precipitation processes on the analysed time scale. The errors are estimated by a Monte Carlo model, which uses a pseudo random number generator that is able to produce random numbers for a given statistical distribution (Scheirer 2001). Therefore, both the shape of mixed distributions and the frequency of precipitation measurements are taken into account. That gives the relative error as a function of the number of measurements for each grid box, as well as the corresponding statistical distribution (Fig. 10, triangles). For comparison we also show the mean errors of the parameters of the main population (crosses) and the corresponding empirical error function (straight line). The variability in the relative error estimates for every grid box can be explained by a sampling error due to the small number of measurements,

and by the spatial variability of measured processes. The error is associated primarily with the number of measurements and, to a lesser degree, is influenced by the mean and frequency of the mixed distribution. The kriging method requires the minimisation of sampling errors and the assessment of the standard error in the units of the covariance. According to Aitchison and Brown (1963), the estimate of the standard error is obtained from

$$\text{Var}[E(\text{rr})] = p^2 \frac{\alpha}{n_r} \left(\sigma^2 + \frac{\sigma^4}{2} \right) + \alpha^2 \frac{p(1-p)}{n_0 + n_r}, \tag{12}$$

where α denotes the expected value of R in the mixed lognormal distribution

$$\alpha = \exp\left(\mu + \frac{\sigma^2}{2}\right) \tag{13}$$

and σ^2 is the variance of the transformed data. The standard errors are estimated from the measurements within each grid box as well as on the basis of the statistical parameters available from the first guess fields after the use of Monte Carlo method (Fig. 11). The correlation coefficient is equal to 0.84. Differences are associated mostly

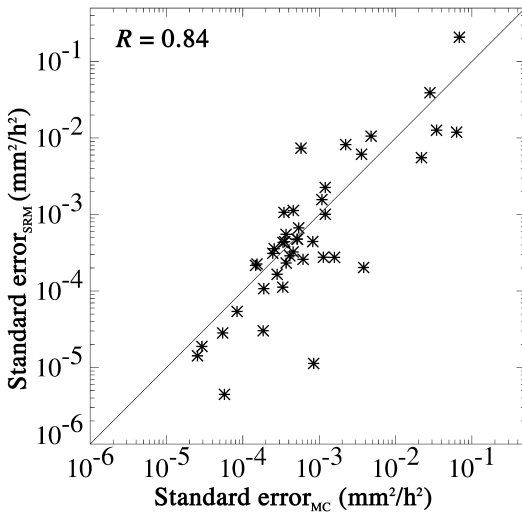


Fig. 11. Comparison of the estimated standard errors based on Monte Carlo simulations and measurements made by the ship rain gauges during autumn 1998. Units are $\text{mm}^2 \text{h}^{-2}$.

with the undersampling of measured data in the areas where the estimates of the distribution parameters are not significant. In order to ensure that the error is not underestimated, the maximum value of the both estimates is used in the Eq. 7 for the computation of the resulting rain amount.

Spatial structure functions

The spatial structure functions needed for the interpolation were estimated on the basis of the first-guess fields mentioned above. Therefore, the weighted means were grouped into equidistant pairs and correlations for each single station-to-station distance were calculated. Due to the small number of grid values available for each individual season, the correlations were calculated from climatological data. The interseasonal variability of the structure functions was less pronounced than the spatial variability estimated on a 8-minute time scale. An example of a nonlinear structure function, fitted to estimated correlation coefficients for the autumn 1998, is given in Fig. 12. The error bars denote the 95% confidence intervals. In comparison to other estimates, the functions seem to provide somewhat

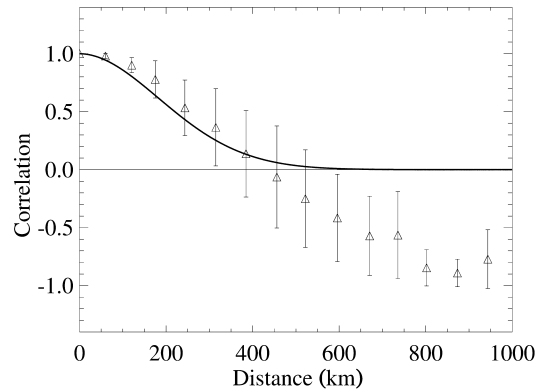


Fig. 12. Climatological structure function for autumn 1998 derived from first guess fields of autumn for the years 1996–2000. The triangles denote the estimated correlation coefficients of the station-to-station distances and the solid line is the empirical correlation function. Error bars mark the 99% confidence intervals of the corresponding correlation.

shorter correlation scale (Rubel 1994). This fact can be explained by the small horizontal dimensions of the Baltic Sea and the large influence of the rain characteristics of the surrounding land masses on seasonal precipitation processes.

Resultant kriging fields

Application of the kriging method according to Eqs. 6–11 results in interpolated precipitation fields with a minimised random distributed error. The weights were calculated with respect to the structure function and random sampling. Thus, the resultant precipitation amounts for the grid boxes analysed accounted for both the averaged raw data and the estimated sampling error with respect to the number of measurements and probability distribution parameters. The standard errors were normalised with respect to the spatial correlation function.

In comparison with the first-guess field for the autumn 1998, the interpolated field (Fig. 13) depicts that the maximum precipitation rates over the south of the Baltic Sea were slightly shifted to the west and had a less pronounced maximum in the central basin. The minimum was found near the Finnish coast. The kriging variance in terms of the relative error gave minimum values

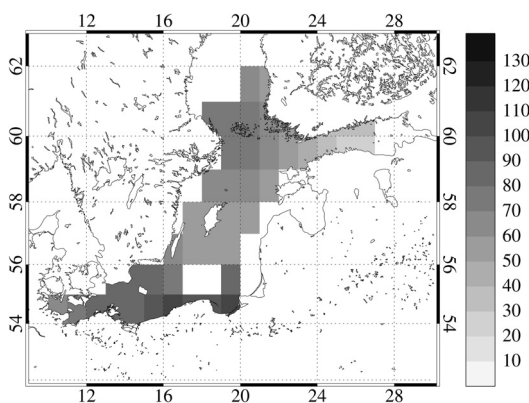


Fig. 13. Interpolated precipitation field (mm month^{-1}) for autumn 1998 using kriging method for minimisation of sampling errors. Units are .

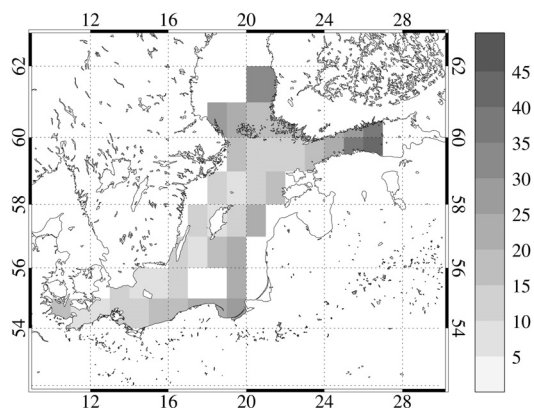


Fig. 14. Relative interpolation error (%) of the analysed precipitation field for autumn 1998.

along the main shipping routes corresponding to a larger number of measurements (Fig. 14). The mean error varied within the range of about 15%–25%. The largest relative error occurred in areas having the lowest data density, especially in the south-east part and over the Gulf of Finland in the north-east part. The analysis of the remainder seasons during the period 1996–2000 gave similar results.

Discussion and conclusions

The presented analysis of the measured rain data gives insight on the seasonal precipitation over the Baltic Sea Proper. The main problem in analysing precipitation measurements from moving ships is that these data are inhomogeneously distributed in space and time, and that the data density is generally low. It is shown that an improved kriging method is suitable for minimising errors due to undersampling. Furthermore, this method gives an estimate of the quality of the resulting precipitation field in terms of the kriging variance. These error estimates showed that even the use of five ships for rain measurements is sufficient to compute precipitation fields on a seasonal timescale. However, they clearly depict also that a large number of measurements is required to analyse precipitation fields on a finer temporal and spatial resolution.

References

- Aitchison J. & Brown J. 1963. *The lognormal distribution*, Cambridge University Press, New York, 176 pp.
- Bacchi B. & Kottogoda N.T. 1995. Identification and calibration of spatial correlation patterns of rainfall. *J. Hydrol.* 165: 311–348.
- Creutin J. & Obled C. 1982. Objective analysis and mapping techniques for rainfall fields: An objective comparison. *Water Resour. Res.* 18: 413–431.
- Dorman C.E. & Bourke R.H. 1978. A temperature correction for Tucker's ocean rainfall estimates. *Quart. J. Met. Soc.* 104: 765–773.
- Frei C. & Schär C. 1998. A precipitation climatology of the Alps from high-resolution rain-gauge observations. *J. Climatol.* 18: 873–900.
- Gandin L. 1965. Objective analysis of meteorological fields. *Gidrometeorologicheskoe Izdatel'stvo (GIMIZ)*. [Translated from Russian by R. Hardin, Israel Program for Scientific Translations, Jerusalem], 242 pp.
- Großklaus M., Uhlig K. & Hasse L. 1998. An optical disdrometer for use in high wind speeds. *J. Atmos. Oceanic Technol.* 15: 1051–1059.
- Hall A. & Barklay P. 1975. Methods of determining areal rainfall from observed data. In: Chapman X. & Dunin X. (eds.), *Prediction in catchment hydrology*, Aust. Acad. Sci., Canberra, 498 pp.
- Hasse L., Großklaus M., Uhlig K. & Timm P. 1998. A ship rain gauge for use under high wind speeds. *J. Atmos. Oceanic Technol.* 15: 380–386.
- Isemer H. 1996. *Weather patterns and selected precipitation records in the PIDCAP period, August to November 1995*. GKSS 96/E/55, GKSS Research Center, Geesthacht, Germany, 92 pp.
- Isemer H. & Lindau R. 1998. Climatological estimates of precipitation and evaporation over the Baltic Proper based on COADS. In: *Conference Proceedings of the*

- Second Study Conference on BALTEX*, International BALTEX Secretariat Publications, 251 pp.
- Kedem B., Chiu L. & North G. 1990. Estimation of mean rain rates: Application to satellite observations. *J. Geophys. Res.* 95: 1965–1972.
- Matheron G. 1963. Principles of geostatistics. *Economic Geology* 58: 1246–1266.
- Michelson D.B., Andersson T., Koistinen J., Collier C.G., Riedl J., Szturc J. & Gjertsen U. 2000a. *BALTEX radar data centre products and their methodologies*. RMK 90, SMHI, Norrköping, Sweden, 76 pp.
- Michelson D.B., Foltescu V.L., Häggmark L. & Lindgren B. 2000b. MESAN mesoscale analysis of precipitation. *Meteorol. Z.* 9: 85–96.
- Omstedt A., Gustafsson B., Rodhe J. & Walin G. 2000. Use of Baltic Sea modelling to investigate the water cycle and heat balance in GCM and regional climate models. *Clim. Res.* 15: 95–108.
- Obled C. & Creutin J. 1986. Some developments in the use of empirical orthogonal functions for mapping meteorological fields. *J. Climate Appl. Meteor.*: 1189–1204.
- Reed R.K. & Elliot W.P. 1973. Precipitation at ocean weather stations in the North Pacific. *J. Geophys. Res.* 78: 7087–7091.
- Reed R.K. & Elliot W.P. 1977. A comparison of oceanic precipitation as measured by gage and assessed from weather reports. *J. Appl. Meteor.* 16: 983–986.
- Rubel F. 1994. *Diagnose vertikaler Niederschlagsflüsse*. Ph.D. thesis, University Vienna, 173 pp.
- Rubel F. 1996. PIDCAP-quick look precipitation atlas. *Österreichische Beiträge zu Meteorologie und Geophysik* 15, Institute for Meteorology and Geophysics, University of Vienna, 95 pp.
- Rubel F. 1998. Ground truth precipitation atlas. *Österreichische Beiträge zu Meteorologie und Geophysik* 18, Institute for Meteorology and Geophysics, University of Vienna, 76 pp.
- Rubel F. & Hantel M. 1999. Correction of daily rain gauge measurements in the Baltic Sea drainage basin. *Nordic Hydrology* 30: 191–208.
- Rutgersson A., Bumke K., Clemens M., Foltescu V., Lindau R., Michelson D. & Omstedt A. 2001. Precipitation estimates over the Baltic Sea: Present state of the art. *Nordic Hydrology* 32: 285–314.
- Scheirer R. 2001. *Solarer Strahlungstransport in der inhomogenen Atmosphäre*. Ph.D. thesis, Institut für Meereskunde, Kiel, 113 pp.
- Simmer C. 1996. Retrieval of precipitation from satellites. In: Raschke E. (ed.), *Radiation and water in the climate system*. NATO ASI Series I: *Global Environmental Change* 45, Springer Verlag, pp. 249–276.
- Skomorowski P., Rubel F. & Rudolf F. 2001. Verifications of GPCP-1DD global satellite precipitation products using MAP surface observations. *Phys. Chem. Earth (B)* 26: 403–409.
- Tucker G.B. 1961. Precipitation over the North Atlantic Ocean. *Quart. J. Met. Soc.* 87: 147–158.
- Vermehren K. 1995. *Bestimmung des Niederschlags auf See aus Wetterbeobachtungen*. Diplomarbeit. Institut für Meereskunde, Kiel, 63 pp.

Received 23 January 2002, accepted 23 September 2002